

## The virial coefficients of the pearl-necklace model

C. Vega, J. M. Labaig, L. G. MacDowell, and E. Sanz

*Departamento de Química Física, Facultad de Ciencias Químicas, Universidad Complutense, 28040 Madrid, Spain*

(Received 20 July 2000; accepted 14 September 2000)

We consider the virial coefficients of an idealized model polymer under good solvent conditions, the so-called pearl-necklace model, consisting of a fully flexible chain of  $m$  tangent hard spheres. We employ an efficient algorithm recently proposed to determine the second, third, and fourth virial coefficients of chains of up to 100 monomers. We also include some preliminary results for chains of up to 200 monomers. These results, which include the first off-lattice calculations of third and fourth virial coefficients of polymer models, are compared with predictions obtained from Wertheim's equation of state. It is shown that, despite the good agreement of Wertheim's equation of state for the compressibility factor, the predictions for the individual virial coefficients are far from satisfactory. It is shown that for the values of  $m$  considered in this work, the truncated virial expansion correctly describes the equation of state up to packing fractions of 0.25. A new equation of state which describes the low and high density regimes of the pearl-necklace model is proposed.

© 2000 American Institute of Physics. [S0021-9606(00)50946-5]

### I. INTRODUCTION

In the last two decades, the interest in the study of flexible molecules from the point of view of statistical thermodynamics has increased considerably. One of the simplest models of a flexible molecule is the pearl-necklace model, in which the polymer is described by  $m$  tangent hard spheres with bond length equal to the diameter of the spheres,  $\sigma$ . As there is no constraint of the bond angle, the molecule is very flexible and may adopt many different configurations. A two-dimensional sketch of the pearl-necklace model is presented in Fig. 1(a). As both the inter- and intramolecular interactions between sites are considered to be of the hard-sphere type, the model describes approximately the interactions between polymer molecules under good solvent conditions.

A somewhat related model is that formed by  $m$  tangent hard spheres in a linear rigid configuration. The bond angle is fixed to  $180^\circ$  and the molecule presents no flexibility. We shall denote this model as the linear tangent hard-sphere model (LTHS). A sketch of this model is presented in Fig. 1(b). This model represents the opposite of the pearl-necklace model since it is fully rigid.

Given the simplicity of the pearl-necklace model, it has played a central role in the study of flexible molecules and for this reason it has been considered in several studies. It is almost impossible to provide an exhaustive list of all the articles devoted to this model, and for this reason we shall provide just a few references. The goal of many of these studies was the search for an equation of state. We should mention the important simulations in this area performed by Hall and co-workers and by Sandler and co-workers.<sup>1-3</sup> Also the fluid-solid equilibrium of this model has been determined via computer simulation for short chains.<sup>4</sup> The search for a theoretical equation of state for this model has also been considered by a number of authors. In the late 1980s, Wertheim<sup>5</sup> and Chapmann, Jackson, and Gubbins<sup>6</sup> proposed

a theoretical equation of state for this model. Two other theoretical equations of state should also be mentioned; the Generalized-Flory dimer theory of Honnell and Hall<sup>7</sup> and the equation of state of Chiew.<sup>8</sup> Also the structure of the pearl-necklace model as given by the average site-site correlation function has been studied in detail. Simulation studies of the site-site correlation function have appeared.<sup>9</sup> In addition to this, integral equations have also been proposed to determine the site-site correlation function of the pearl-necklace model. We should mention the theoretical studies of Curro and Schweizer,<sup>10</sup> Chiew,<sup>11</sup> Chang and Sandler,<sup>12</sup> and Lin *et al.*<sup>13</sup>

Somewhat surprisingly, the virial coefficients of the pearl-necklace model have not been studied in such detail. Only the second virial coefficient of the pearl-necklace model has been determined numerically by Yethiraj *et al.*<sup>14</sup> and Wichert and Hall.<sup>15</sup> Very little is known about the higher virial coefficients of this model. The main goal of this study is to provide data on the third and fourth virial coefficients. This is interesting *per se* and also serves to test the performance of the theoretical equations of state in the low density regime.

The numerical determination of the third and fourth virial coefficient of a flexible molecule, however, appears as a nontrivial problem. We have recently presented an algorithm to evaluate virial coefficients of any multicomponent system.<sup>16</sup> We treat the flexible molecule as a multicomponent mixture, where each possible configuration of the polymer represents a different component. In this work, we apply this algorithm to the pearl-necklace model, obtaining for the first time the third and fourth virial coefficients of a flexible model in the continuum. To the best of our knowledge, the only previous study related to this problem is that of Bruns, where the third virial coefficient of a polymer molecule on a lattice was determined numerically.<sup>17</sup> The virial coefficients obtained in this work will be compared with the theoretical

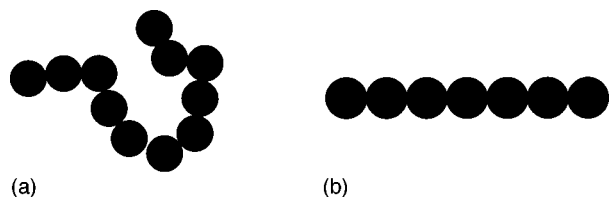


FIG. 1. (a) Sketch of an instantaneous configuration of the pearl-necklace model. (b) The linear tangent hard-sphere (LTHS) model.

predictions of the equation of state (EOS) proposed by Wertheim, which is known as the first order perturbation theory (TPT1). One of the goals of this work is to check whether this successful equation of state is also successful in the prediction of the virial coefficients of these systems. It will be shown that TPT1 yields poor predictions for the virial coefficients.

Another interesting question is the accuracy of the virial expansion for describing the equation of state of a hard flexible model. It is clear that a truncated virial expansion cannot describe the equation of state of any hard model over all the density range. However, it is difficult to know exactly at which packing fraction will this oversimplified description fail. We will analyze this issue. It will be found that the virial expansion truncated at the fourth virial coefficient describes reasonably well the equation of state of the pearl-necklace model up to volume fractions of about 0.25, at least for the chains considered in this work (i.e., those with  $m$  less than 100). Finally, we shall propose a new equation of state which will improve the performance of TPT1 at low densities.

The scheme of the article is as follows: in Sec. II the method used to determine the virial coefficients will be briefly described. In Sec. III, the virial coefficients as predicted by Wertheim TPT1 EOS will be presented. In Sec. IV the results for the virial coefficients of the pearl-necklace model will be presented, and in Sec. V the main conclusions to this work will be given.

## II. NUMERICAL DETERMINATION OF THE VIRIAL COEFFICIENTS

The pressure of a homogeneous isotropic fluid can be given in terms of a power series of the density by the following expression:

$$Z = \frac{P}{\rho kT} = 1 + B_2(T)\rho + B_3(T)\rho^2 + B_4(T)\rho^3 + \dots, \quad (1)$$

where  $\rho$  is the number density (number of molecules per unit volume) of the system and the coefficients  $B_2$ ,  $B_3$ , and  $B_4$  are the second, third, and fourth virial coefficients, respectively.

As can be seen from the above equation, the virial coefficients are generally temperature dependent. However, if all interactions in the system are of hard type (i.e., the pair potential is either zero or infinity), as is the case in the pearl-necklace model, the virial coefficients are no longer temperature dependent. In such cases, it is more convenient to

express the virial series [Eq. (1)] in terms of the packing fraction, which is a reduced density given in units of the molecular volume:

$$Z = 1 + B_2^*y + B_3^*y^2 + B_4^*y^3 + \dots, \quad (2)$$

where the reduced virial coefficients,  $B_n^*$ , are defined as  $B_n^* = B_n/V_m^{n-1}$ , while  $y = \rho V_m$  is the packing fraction and  $V_m$  is the molecular volume. In the case of the pearl-necklace model made of  $m$  tangent hard spheres,  $V_m = m\pi\sigma^3/6$ .

The link between the macroscopic expression given by Eq. (1) and the microscopic world was made in the 1930s, when it was shown that the virial coefficients could be given in terms of certain integrals involving the potential energy between molecules. As the expressions in terms of these integrals may become rather lengthy, it has become customary to represent them by graphs. In terms of these graphs, the third and fourth virial coefficients of a rigid molecule are given by<sup>18-20</sup>

$$B_3 = -\frac{1}{3V} \text{ (triangle graph) } \quad (3)$$

$$B_4 = -\frac{1}{8V} \left( \text{tetrahedron graph} + 6 \text{ (square graph)} + 3 \text{ (rectangle graph)} \right). \quad (4)$$

In these graphs, solid lines represent Mayer functions,  $f = \exp(-\beta u) - 1$ , where  $\beta = 1/(kT)$  and  $u$  is the pair potential between pairs of molecules. On the other hand, black circles represent integration with respect to the coordinates of the corresponding molecule.

The extension of this notation to multicomponent systems or systems made of flexible molecules has been considered recently.<sup>16</sup> Actually, it suffices to consider that, for each of the black circles representing a given molecule, there is a corresponding singlet correlation function which describes the probability of occurrence of that molecule in the system. In the case of a multicomponent mixture, this probability will be simply given by the arbitrarily fixed molar fractions of the mixture, while in the case of a flexible molecule, it will be given by the corresponding Boltzmann weight of each of the conformers.

We shall evaluate the virial coefficients by following the method described in Ref. 16. We shall provide an outline of the procedure here, though the reader is recommended to read the reference for a much fuller description. In the first stage, a conventional Monte Carlo procedure is performed in order to obtain a sample of conformers chosen with a probability proportional to their Boltzmann weights. The chemical identity of each of the molecules required in the evaluation of the graphs is then selected at random from the sample. For this given set of conformers, each of the graphs is evaluated using the procedure of Ree and Hoover,<sup>21</sup> as explained in Ref. 16. The final value for the virial coefficients of the chain molecules is then obtained as an average of the virial coefficients over the possible sets of two, three, four, or more conformers required in the corresponding graphs.

The conformers which form the sample were obtained by means of a conventional single chain Monte Carlo simulation, using the reptation algorithm.<sup>22</sup> The simulations in-

volved about 80 million steps for equilibration, followed by a further 160 million steps for the production of the sample. Once the system was equilibrated, the instantaneous configuration of the chains were stored in a file every 160 000 time steps, producing a sample with a total of 1000 independent instantaneous configurations. From this sample,  $N_{\text{chemical}} = 400$  tetrads of conformers chosen at random were used to evaluate the average virial coefficient of the chain molecules. For each of the tetrads, the graphs were evaluated by averaging over a total of  $N_{\text{orien}} = 80\,000$  orientations of the corresponding conformers in that tetrad. This procedure was repeated four times, in order to get four uncorrelated average values for the virial coefficients.

The numerical determination of  $B_3$  and  $B_4$  for a short chain with  $m = 7$  takes only a few hours on a Pentium III 450 MHz personal computer. However, calculations for  $m = 100$  would take around 200 days on a Pentium III 450 MHz computer. Therefore, calculations for long-chain molecules were performed on an Origin 2000 computer in the University Complutense Computer Center. Running on a single processor, bench marks suggested that the same calculation would last 100 days on this machine (i.e., the SGI R10000 processor doubles the speed of the Pentium machine). We therefore wrote a parallel version of our program and executed it on the Origin 2000, using 10 processors simultaneously. Results for  $m = 100$  were then obtained in just 11 days! Therefore, with the currently available computers, calculations of virial coefficients for long polymers (i.e.,  $m$  larger than 100) can be performed only on parallel machines.

### III. THEORETICAL PREDICTIONS FOR THE VIRIAL COEFFICIENTS

In this work we shall consider the predictions of the virial coefficients as obtained from the thermodynamic perturbation theory of first order (TPT1), first proposed by Wertheim<sup>5</sup> and Chapman, Jackson, and Gubbins.<sup>6</sup> The TPT1 equation of state reads

$$Z_{\text{TPT1}} = m \frac{1 + y + y^2 - y^3}{(1 - y)^3} - (m - 1) \frac{1 + y - y^2/2}{(1 - y)(1 - y/2)}, \quad (5)$$

where  $y$  is the volume fraction. As can be seen, this equation of state predicts that for a certain volume fraction the compressibility factor is a linear function of  $m$ . The virial coefficients arising from TPT1 were first obtained by Boublik.<sup>23,24</sup> They are given by the following expressions:

$$B_2^{*,\text{TPT1}} = 2.5 + 1.5m, \quad (6)$$

$$B_3^{*,\text{TPT1}} = 2.75 + 7.25m, \quad (7)$$

$$B_4^{*,\text{TPT1}} = 2.875 + 15.125m. \quad (8)$$

As can be seen, the virial coefficients arising from TPT1 are linear functions of  $m$ . This is a consequence of the fact that TPT1 predicts a linear dependence of  $Z$  on  $m$  for a given value of  $y$ .

TABLE I. Second, third, and fourth virial coefficients for the pearl-necklace model as obtained in this work by the exact procedure described in Sec. II. We use the parameters  $N_{\text{orien}} = 80\,000$  and  $N_{\text{chemical}} = 1600$ , except for  $m = 150, 200$  where we used  $N_{\text{chemical}} = 800$  (see Ref. 16 for the notation). Results labeled with an asterisk were obtained by using the approximated method described in Sec. IV. The numbers in parentheses give the uncertainty of the last digits. Values of the mean-square radius of gyration  $\langle s^2 \rangle$  are given in the last column.

$m$	$B_2^*$	$B_3^*$	$B_4^*$	$\langle s^2 \rangle$
7	10.18(5)	53.2(1)	139(1)	1.740
10	12.51(7)	77.4(6)	214(1)	2.857
16	16.74(8)	132(1)	381(4)	5.403
16*	16.71(8)	132(1)	361(6)	5.403
32	26.1(2)	302(3)	881(20)	13.424
64	42.1(1)	743(3)	1885(150)	32.419
64*	42.0(1)	744(3)	1356(140)	32.419
100	57.9(4)	1355(15)	2203(500)	56.568
150	76.92(6)	2357(30)	1563(800)	93.21
200	95.28	3552	-2637	132.40

## IV. RESULTS

### A. Comparing exact virial coefficients with predictions from TPT1

In Table I we collect the second, third, and fourth virial coefficient of the pearl-necklace model for  $m = 7, 10, 16, 32, 64,$  and  $100$ . In order to clarify the role of flexibility, we have also evaluated the virial coefficients of the LTHS model. In Table II, the numerical results obtained in this work are presented. Virial coefficients of the LTHS model were calculated previously by Vega *et al.*<sup>25</sup> for short chains with  $m$  up to 8, and here we extend the calculations to longer chains.

In Fig. 2, the second virial coefficients of the pearl-necklace model as obtained numerically in this work are compared with those predicted by TPT1. As can be seen, the predictions of TPT1 are rather poor. According to TPT1,  $B_2^*$  increases linearly with  $m$ . However, it is well-known<sup>26-29</sup> that the reduced second virial coefficient of hard polymer molecules with intramolecular and intermolecular hard interactions (i.e., good solvent conditions) scale as  $m^{3\nu-1} \approx m^{0.8}$ , where  $\nu$  is the exponent describing the scaling of the mean-square radius of gyration of the molecule (i.e.,  $\langle s^2 \rangle \propto m^{2\nu}$ ). Therefore, the second virial coefficient of the pearl-necklace model increases more slowly than linearly and accordingly, TPT1 significantly overestimates the second virial coefficient. This, in fact, has already been illustrated by Yethiraj *et al.*<sup>14</sup> Where available, the second virial coefficients obtained previously by Yethiraj *et al.*<sup>14</sup> have also been

TABLE II. Second, third, and fourth virial coefficients for the LTHS model as obtained in this work by the exact procedure described in Sec. II. The numbers in parentheses give the uncertainty of the last digits.

$m$	$B_2^*$	$B_3^*$	$B_4^*$
7	12.427(9)	58.43(7)	42(1)
10	16.61(2)	87.2(2)	-62(4)
20	30.45(4)	195.1(5)	-1284(15)
30	44.32(4)	317(2)	-4051(49)
50	72.18(6)	585(4)	-15 481(256)
100	141.3(5)	1338(22)	-77 055(4039)

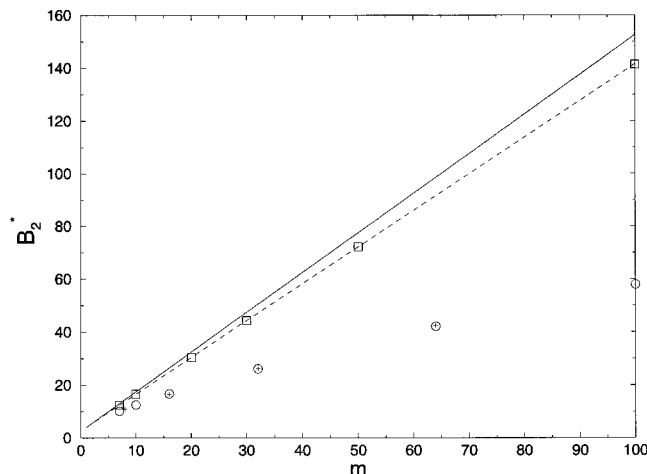


FIG. 2. Reduced second virial coefficient  $B_2^*$  for hard models made up of  $m$  tangent hard spheres. Numerical results of this work for the pearl-necklace model (open circles), numerical results for the pearl necklace model from Yethiraj (Ref. 14) (plus sign), Wertheim TPT1 predictions (solid line), numerical results of this work for the LTHS model (open squares), exact predictions (Refs. 30, 31) for the LTHS (dashed line).

included in Fig. 2. As can be seen, the results of this work for  $B_2^*$  are in good agreement with those of Yethiraj *et al.*

In Fig. 2, the second virial coefficients of the LTHS model are also presented. Symbols are results of this work, while the straight line is the exact value, which has been determined by Williamson and Jackson<sup>30</sup> and Sullivan *et al.*<sup>31</sup> These authors have shown that for large molecules, the second virial coefficient of the LTHS becomes a linear function of  $m$ . As can be seen, the numerical results of this work agree with the exact analytical value.

The results of Fig. 2 allow one to arrive at several conclusions. Rigid and flexible models differ significantly in the second virial coefficient. According to TPT1, the virial coefficients of any model made up of tangent hard spheres will have the same equation of state and hence the same virial coefficients. As it is shown in Fig. 2, this is not correct, since virial coefficients are sensitive to differences in the structure of the molecule. The slope of  $B_2^*$  vs.  $m$  is 1.388 for the LTHS, whereas TPT1 predicts this slope to be 1.5. Therefore, TPT1 does not correctly predict the second virial coefficient neither for rigid nor for flexible models of tangent hard spheres.

In Fig. 3, results for  $B_3^*$  are presented. It can be seen that flexible and rigid linear chains do not differ significantly in the third virial coefficients. Thus, we can conclude that the third virial coefficient is not sensitive to details in the molecular structure, in agreement with the predictions of TPT1. However, TPT1 is not satisfactory from a quantitative point of view. In fact, the third virial coefficient is underestimated significantly when compared to the exact results.

In Fig. 4, results for  $B_4^*$  are presented. Again, at the fourth virial coefficient level there are significant differences between flexible and rigid models, though TPT1 is not accurate at predicting the fourth virial coefficient, neither for the flexible chains nor for the rigid ones. As can be seen in the figure, the fourth virial coefficient of the LTHS becomes negative for  $m$  larger than 8. This might have been expected,

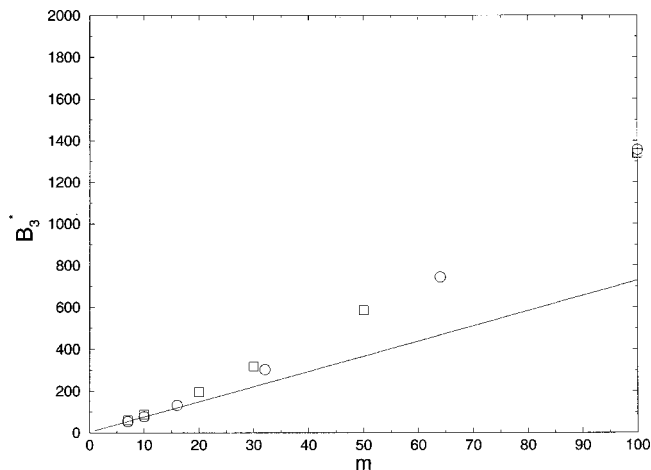


FIG. 3. Reduced third virial coefficient  $B_3^*$  of models formed by  $m$  tangent hard spheres. Numerical results of this work for the pearl-necklace model (open circles), Wertheim's TPT1 predictions (solid line), numerical results of this work for the LTHS model (open squares).

since rigid prolate molecules such as spherocylinders and ellipsoids reach negative values of  $B_4^*$  for length-to-breadth ratios larger than 8, approximately. The LTHS is not an exception to this general rule. On the other hand, for the pearl-necklace model, the fourth virial coefficient is positive for values as large as  $m=100$ . However, it should be noted, though not included in the figure, that there is some evidence that  $B_4^*$  may actually reach a maximum value and then decrease for long polymer chains, possibly reaching negative values. This evidence comes from the preliminary results shown in Table I for virial coefficients of chains of  $m=150$  and 200. We should mention that for these lengths, however, our results are merely orientative, as they are affected by extremely large error bars. The accurate calculation of  $B_4$  for  $m=150,200$  is, at this time, beyond the capability of currently available supercomputers.

From the results of Figs. 2–4 one may conclude that TPT1 does a poor job in predicting the virial coefficient of flexible or rigid tangent hard spheres models. This is not to

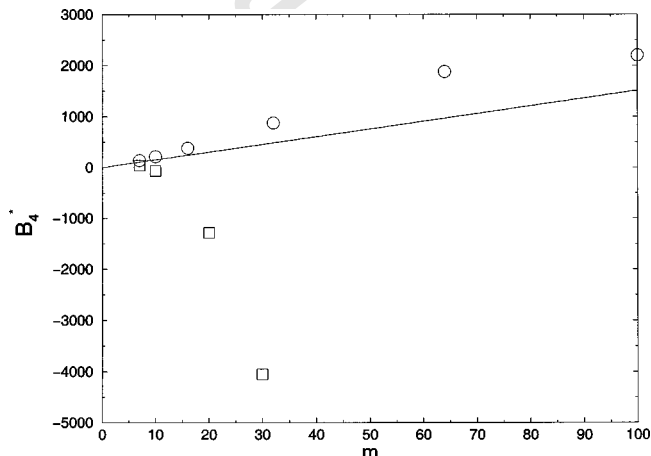


FIG. 4. Reduced fourth virial coefficient  $B_4^*$  of models formed by  $m$  tangent hard spheres. Numerical results of this work for the pearl-necklace model (open circles), Wertheim's TPT1 predictions (solid line), numerical results of this work for the LTHS model (open squares).

say that TPT1 is a bad EOS. In fact, for the pearl-necklace model TPT1 overestimates the values of  $B_2^*$ , but underestimates the value of  $B_3^*$  and  $B_4^*$  (at least for  $m < 100$ ). Therefore, the good predictions of TPT1 at moderate densities arise from a fortuitous cancellation of errors.

## B. Scaling laws for the virial coefficients

Having presented the virial coefficients for the pearl-necklace model, we shall now analyze their scaling laws.

According to the scaling hypothesis,<sup>26</sup> the pressure of a flexible chain molecule can be expressed as

$$Z = F(\rho/\rho_c), \quad (9)$$

where  $\rho_c$  is defined as the concentration at which the polymer coils start to overlap with each other (i.e.,  $\rho_c \propto 1/\langle s^2 \rangle^{3/2} \propto m^{-3\nu}$ ). Therefore, according to the scaling hypothesis,

$$Z = F(\rho m^{3\nu}). \quad (10)$$

A Taylor expansion in powers of the density then shows that the virial coefficients of a polymer should scale as

$$B_n \propto m^{3(n-1)\nu}. \quad (11)$$

For the second virial coefficient, the validity of Eq. (11) has been tested in a number of studies, while for the third virial coefficient, Eq. (11) has been analyzed for lattice chains with up to  $m = 65$ .<sup>17</sup> Unfortunately, the chains considered in this work are not long enough to test Eq. (11) directly. However, an indirect way of testing Eq. (11) is by realizing that it implies

$$\lim_{m \rightarrow \infty} \frac{B_3}{B_2^2} = \frac{B_3^*}{(B_2^*)^2} = g = \text{constant}, \quad (12)$$

for large values of  $m$ .

In Fig. 5(a), the ratio given by Eq. (12) is shown as a function of  $m$ , and in Fig. 5(b) as a function of  $1/\sqrt{m}$ . Results are shown for the pearl-necklace model and for the LTHS model. For the pearl-necklace model, we have included data of  $B_3$  for chains with  $m = 150, 200$  (see also Table I). Recall, however, that these data are somewhat less accurate than those for chains with up to 100 monomer units. The reason is that calculations for  $m = 150, 200$  are much more expensive than those of shorter chains and therefore the graph of Eq. (3) can be evaluated much less often.

Let us first discuss the behavior of  $B_3/B_2^2$  for the pearl-necklace model. The results presented in Fig. 5 strongly suggest that, for this model, the ratio  $B_3/B_2^2$  reaches a constant nonzero value for infinitely long chains, in agreement with the predictions from Eq. (12). This work suggests that the value of this ratio, which is commonly denoted as  $g$ , seems to be close to 0.35. On the other hand, Bruns<sup>17</sup> has estimated the value of  $g$  to be of 0.30 for lattice polymer models. Other values of  $g$  have been suggested.<sup>32</sup> Flory<sup>33</sup> advocated the choice  $g = 0.25$ . Berry<sup>34</sup> proposed the value  $g = 0.33$  and renormalization group calculations obtained  $g = 0.277$  or  $g = 0.44$ .<sup>35,36</sup> The value obtained in this work appears as reasonable as compared to these previous estimates. In any case

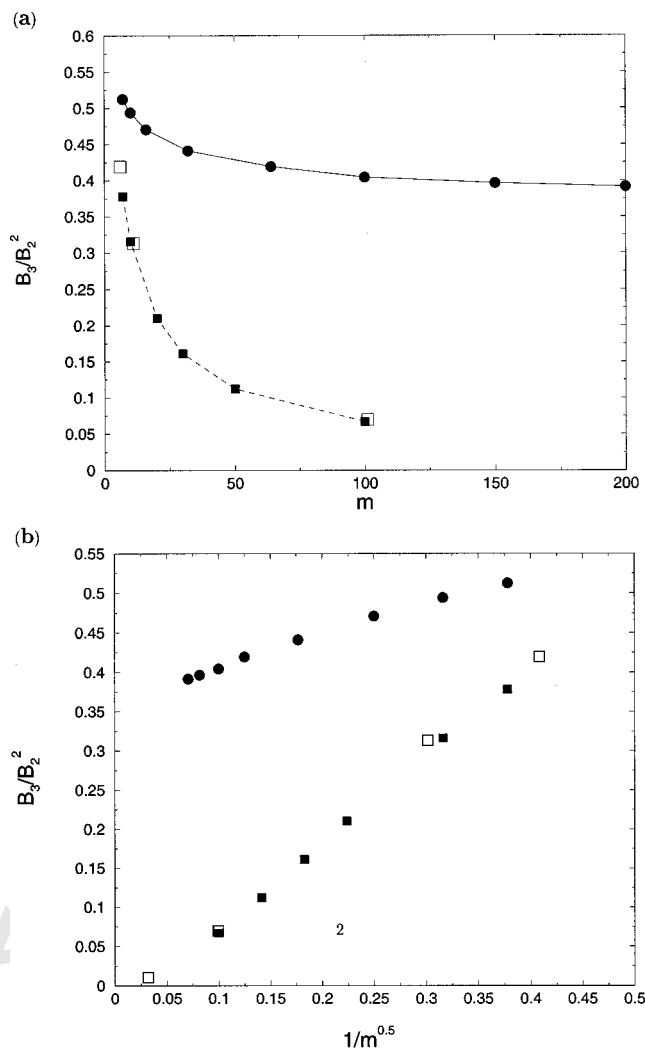


FIG. 5. Value of the ratio  $B_3/B_2^2$  for several hard models. Results for the pearl-necklace model obtained in this work (filled circles), results for the LTHS obtained in this work (filled squares), results for hard spherocylinders taken from Ref. 37 (open squares). (a)  $B_3/B_2^2$  plotted as a function of  $m$ . (b)  $B_3/B_2^2$  plotted as a function of  $1/\sqrt{m}$ .

the results of this work suggest that the scaling hypothesis as represented by Eq. (11) seems to hold for the second and third virial coefficients of flexible chains.

Let us now discuss the behavior of the ratio  $B_3/B_2^2$  for the LTHS. Note that, apart from the results of the LTHS model, we have also included the results for hard spherocylinders (HSC) taken from Frenkel.<sup>37</sup> In order to compare the results from both models in a unified way, the value of  $m$  for the spherocylinder is chosen from that LTHS with equal length-to-breadth ratio. Notice that, when plotted this way, it is seen that the ratio  $B_3/B_2^2$  is almost the same for the LTHS and HSC of the same elongation. It is thus seen that, for rigid linear molecules, the detailed shape of the molecule does not affect strongly this ratio, and only the length-to-breadth ratio matters. Also note that  $B_3/B_2^2$  is clearly seen to vanish as the length of the chains increases. This is in agreement with predictions by Onsager, who conjectured that this ratio should become vanishingly small for linear rigid molecules.<sup>38</sup> This result has been confirmed for HSC,<sup>37</sup> and here we show that it is also obeyed for LTHS.

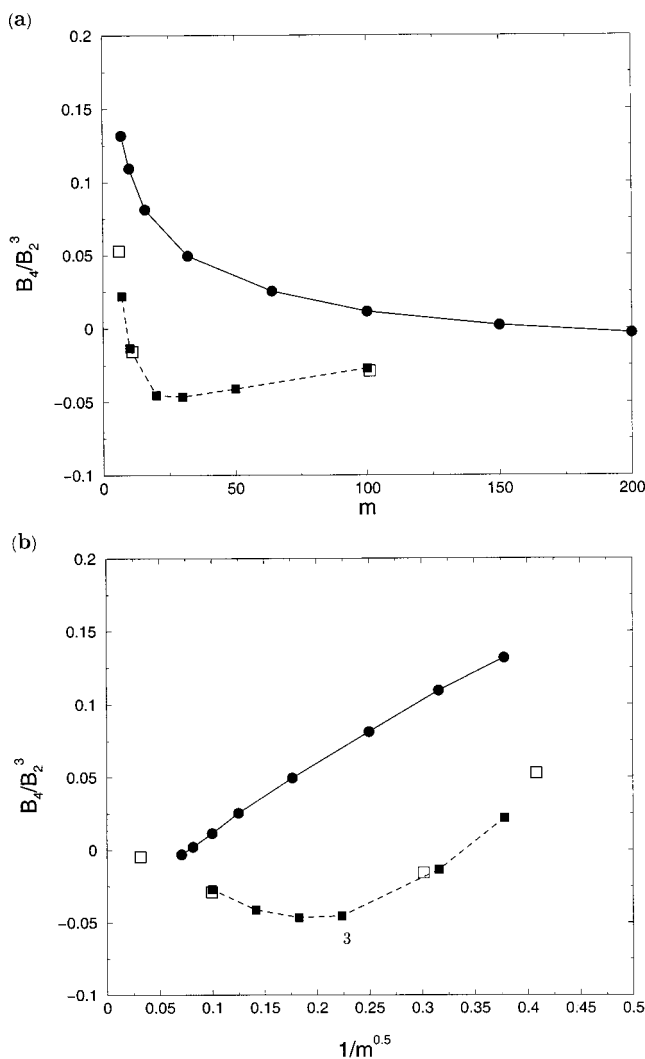


FIG. 6. Value of the ratio  $B_4/B_2^3$  for several hard models. Results for the pearl-necklace model obtained in this work (filled circles), results for the LTHS obtained in this work (filled squares), results for hard spherocylinders taken from Ref. 37 (open squares). (a)  $B_4/B_2^3$  plotted as a function of  $m$ . (b)  $B_4/B_2^3$  plotted as a function of  $1/\sqrt{m}$ .

To summarize, the behavior of  $B_3/B_2^2$  in the limit of infinitely long chains reflects the presence or absence of flexibility in a model. It tends to a value of about 0.35 for flexible chains (i.e., at least for the pearl-necklace model) and to zero for linear rigid molecules. In other words, it can be said that the ratio  $B_3/B_2^2$  in the limit of infinitely large size presents Onsager scaling for rigid molecules and de Gennes scaling for flexible chains. On the other hand, TPT1 predicts that this ratio goes to zero for infinitely large molecules, which is the right behavior for rigid linear molecules but the wrong behavior for flexible ones.

Let us now discuss the scaling law for the fourth virial coefficient. One conclusion of the scaling hypothesis for  $B_4$  is that

$$\lim_{m \rightarrow \infty} \frac{B_4}{B_2^3} = \frac{B_4^*}{(B_2^*)^3} = \text{constant}, \quad (13)$$

for long flexible chains.

In Fig. 6(a), the ratio given by Eq. (13) is shown as a

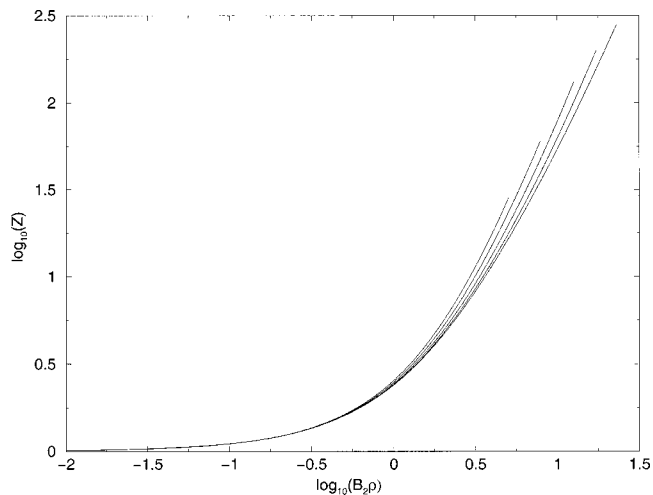


FIG. 7. Verification of the scaling hypotheses [Eq. (10) of main text]. The logarithm of the compressibility factor  $Z$  is plotted as a function of the logarithm of  $B_2\rho$ . Values of  $Z$  were obtained from the truncated (at  $B_4$ ) virial expansion using the virial coefficients determined in this work. Results from top to bottom correspond to  $m=16$ ,  $m=32$ ,  $m=64$ ,  $m=100$ , and  $m=150$ . The maximum density plotted for each model corresponds to  $y=0.30$ .

function of  $m$ , and in Fig. 6(b) as a function of  $1/\sqrt{m}$ . Results are shown for the pearl-necklace model and for the LTHS model. For the pearl-necklace model we have included data for  $B_4$  for chains with  $m=150$  and  $200$  (see also Table I), although we should bear in mind that for these lengths our results just give the order-of-magnitude of  $B_4$ . Let us first discuss the behavior of  $B_4/B_2^3$  for the pearl-necklace model. The results presented in Fig. 6 strongly suggest that for this model, the ratio  $B_4/B_2^3$  reaches a constant value in the limit of long chains. It is hard to decide from our data whether this constant is zero or a small nonzero value. In any case, one may conclude that the limiting value of  $B_4/B_2^3$  for infinitely long flexible chains is quite small. Let us now discuss the results for the LTHS. As can be seen, this ratio seems to go to zero in the limit of infinitely long chains. In Fig. 6 we have also included the results for hard spherocylinders taken from Frenkel.<sup>37</sup> Again, it is seen that the ratio  $B_4/B_2^3$  is almost the same for the LTHS and HSC of the same elongation. It is well-known that for HSC, the ratio  $B_4/B_2^3$  tends to zero for very elongated molecules.<sup>38,37</sup> Therefore, we can conclude that for the LTHS this ratio also goes to zero. Onsager scaling holds for  $B_4$  of rigid chains, and our results suggest that this could also be the case for flexible chains. As to TPT1, it predicts that this ratio goes to zero when  $m$  goes to infinity, both for the flexible and rigid models.

Let us finish this section by analyzing some of the consequences of Eq. (10) (i.e., the scaling hypotheses). It is well-known that under good solvent conditions,  $B_2$  scales as  $m^{3\nu}$ . It then follows from Eq. (10) that  $Z$  must be a universal function of  $\rho B_2$ . In Fig. 7, the value of  $Z$  as obtained from the virial expansion (truncated at  $B_4$ ) is plotted as a function of  $\rho B_2$ . For each model, the highest considered density corresponds to  $y=0.30$ . A similar plot has been recently presented by Lue.<sup>39</sup> As can be seen, all the curves follow onto a universal curve for densities smaller than  $\rho B_2=1$ . For higher

densities, differences appear between the different models, being that the value of  $Z$  for a certain value of  $\rho B_2$  is lower for longer chains. Similar conclusions were obtained by Lue.<sup>39</sup>

### C. Correlation between virial coefficients and single chain properties

The results presented in Table I correspond to the exact numerical determination of  $B_2^*$ ,  $B_3^*$ , and  $B_4^*$ . Since it is the first time that third and fourth virial coefficients have been evaluated for flexible molecules, we would like to analyze the accuracy of other possible approximate methods of evaluating the virial coefficients which have been tested recently.<sup>40</sup> Let us start by showing the exact formulas for the second and third virial coefficient of a multicomponent mixture:

$$B_2 = \sum_i \sum_j x_i x_j B_{ij}, \quad (14)$$

$$B_3 = \sum_i \sum_j \sum_k x_i x_j x_k B_{ijk}, \quad (15)$$

where  $x_i$  is the molar fraction of component  $i$ .

For the pearl-necklace model, we can think of each instantaneous configuration of the isolated chain (free of intramolecular overlap) as a different component. Let us now make an approximation for the crossed virial coefficients  $B_{ij}$  and  $B_{ijk}$ . If we apply the following mixing rules,

$$B_{ij} = (B_{ii} + B_{jj})/2, \quad (16)$$

$$B_{ijk} = (B_{iii} + B_{jjj} + B_{kkk})/3, \quad (17)$$

to Eq. (14) and Eq. (15), they can be rewritten as

$$B_2 = \sum_i x_i B_{ii}, \quad (18)$$

$$B_3 = \sum_i x_i B_{iii}, \quad (19)$$

with an analogous equation for the fourth virial coefficient. Of course Eqs. (18)–(19) are not exact, since they are based on the approximations given by Eqs. (16)–(17). One interesting feature of Eqs. (18)–(19), however, is that they allow one to estimate the average virial coefficients of the chain molecules from the virial coefficients of individual configurations. In this way, the algorithm of Sec. II may be used by selecting a single conformer to compute each of the required graphs.

In Table I, the virial coefficients for  $m=16$  and  $m=64$  obtained in this way are presented (see the results labeled with an asterisk). By comparing the results of Table I obtained with the approximate methodology, with the ones obtained with the exact methodology, one concludes that the approximate method provides accurate estimates of  $B_2$  and  $B_3$  but poor predictions for  $B_4$ . In fact, differences in the fourth virial coefficient are of about 5% for  $m=16$  and of about 30% for  $m=64$ . Clearly, the approximate methodol-

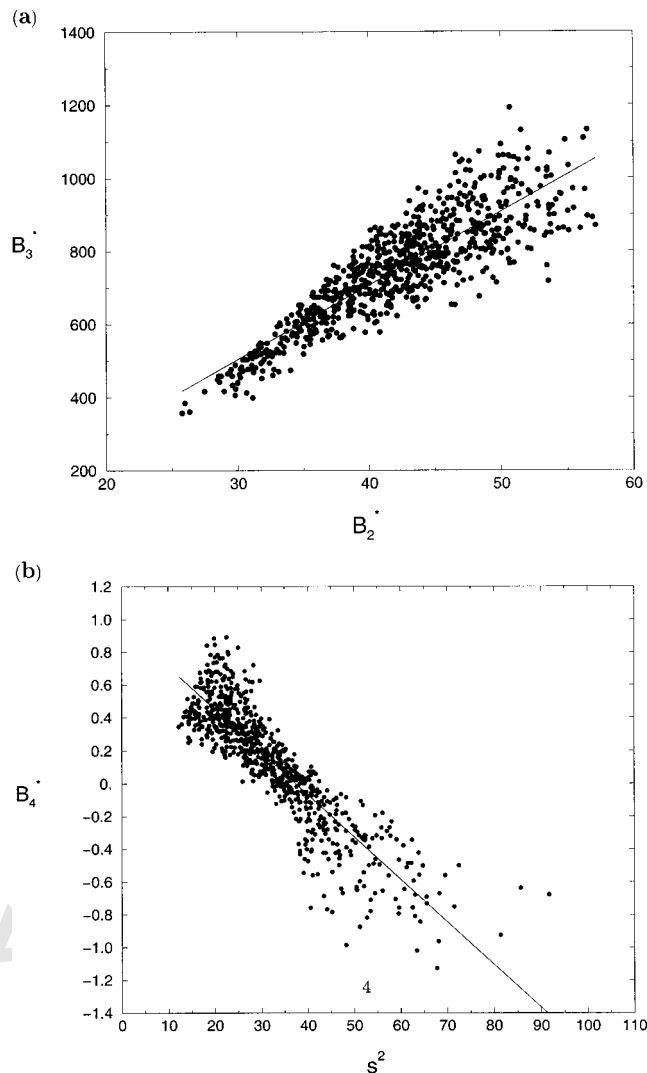


FIG. 8. (a) Correlation between  $B_3$  and  $B_2$  in the pearl-necklace model with  $m=64$  obtained with the approximate methodology. (b) Correlation between  $B_4$  and  $s^2$  for the pearl-necklace model with  $m=64$  obtained with the approximate methodology.

ogy breaks down for the fourth virial coefficients, especially as the chains become longer. One may suspect that the same would occur for higher virial coefficients.

The approximate method has the advantage of allowing a simpler discussion of the virial coefficients of chains. For instance, one may analyze correlations between the individual virial coefficients and single chain properties such as the radius of gyration or even other individual virial coefficients. We shall now analyze the virial coefficients obtained from the approximate methodology for the pearl-necklace model with  $m=64$ . In Fig. 8(a), we present the correlation between the second and third virial coefficient. Results are presented for 800 instantaneous configurations of the pearl-necklace model. As can be seen in Fig. 8(a),  $B_3^*$  and  $B_2^*$  are strongly correlated, with a correlation coefficient of about 0.88. The higher the excluded volume between two molecules (for hard models the second virial coefficient is one-half of the excluded volume),<sup>41</sup> the higher the third virial coefficient. In Fig. 8(b), the correlation between  $B_4^*$  and the radius of gyration,  $s^2$ , is shown. Again, it can be seen that

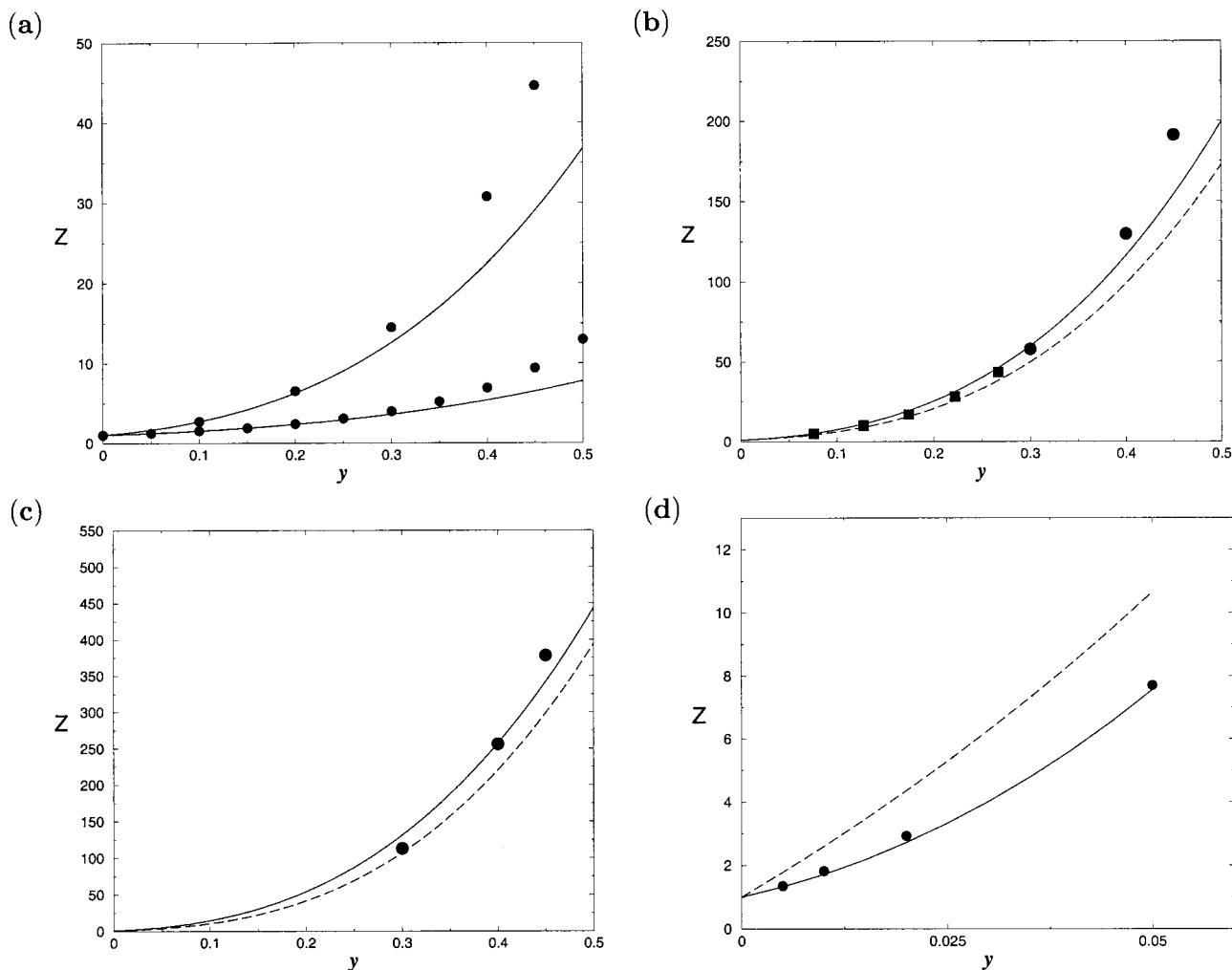


FIG. 9. Compressibility factor of the pearl-necklace model as obtained from computer simulation (Refs. 39, 44) (symbols) and from the truncated (at  $B_4$ ) virial expansion of the pearl-necklace model (solid line). (a) Results for  $m=1$  (bottom) and  $m=7$  (top). (b) Results for  $m=32$ , circles (from Zhou *et al.*, Ref. 44), squares (McBride, Ref. 49). The results of the truncated virial expansion for the SW chain are also shown (dashed line). (c) Results for  $m=64$ . The results of the truncated virial expansion for the SW chain are also shown (dashed line). (d) Results for  $m=100$ . Symbols are simulation results from Lue (Ref. 39). Wertheim's EOS prediction is shown as a dashed line.

these two properties are strongly correlated. In fact, the correlation coefficient of Fig. 8(b) is  $-0.89$ . Also note that, for large values of  $s^2$ ,  $B_4^*$  becomes negative. This is in agreement with the intuitive idea that configurations with larger values of  $s^2$  are somewhat stretched and somehow resemble the shape of a prolate spherocylinder or ellipsoid, for which  $B_4$  becomes negative.<sup>42,43</sup> Figure 8(b) serves also to illustrate the difficulty in accurately evaluating the fourth virial coefficient of long molecules. In fact, when computing  $B_4^*$  for  $m=64$ , we found values from around  $-12\,000$  up to about  $10\,000$  depending on the chosen configuration. Such a big dispersion of the results is reflected in very large error bars, as shown in Table I.

#### D. Equation of state

We shall now focus on the possibility of describing the equation of state of the pearl-necklace model in the low density regime via a virial expansion truncated at the fourth virial coefficient level. In Fig. 9, the EOS of the pearl-necklace model with  $m=1, 7, 32, 64, 100$  as obtained from

computer simulations<sup>44,39</sup> and from the truncated virial expansion is presented. It can be seen that the truncated virial expansion is able to correctly describe the compressibility factor of the pearl-necklace model for volume fractions up to  $y=0.25$ . For larger densities, the truncated virial expansion significantly underestimates the compressibility factor. Obviously, for high densities the contributions from the fifth and the rest of the coefficients of the virial expansion should be included. In Fig. 9(d), a comparison between simulation results<sup>39</sup> for the pearl-necklace model with  $m=100$ , the truncated virial expansion, and Wertheim's EOS is presented. This figure shows clearly the failure of Wertheim's EOS at very low densities (i.e., for  $y<0.10$ ). This failure is expected, since Wertheim's EOS does not correctly predict the virial coefficients as was shown in Figs. 2–4.

Zhou *et al.* have shown by analyzing their simulation results for the pearl-necklace model that the compressibility factor for a fixed value of the volume fraction (i.e.,  $y$ ) becomes a linear function of  $m$  once  $m$  is sufficiently big (typically larger than 7).<sup>44</sup> This seems to be a general trend in

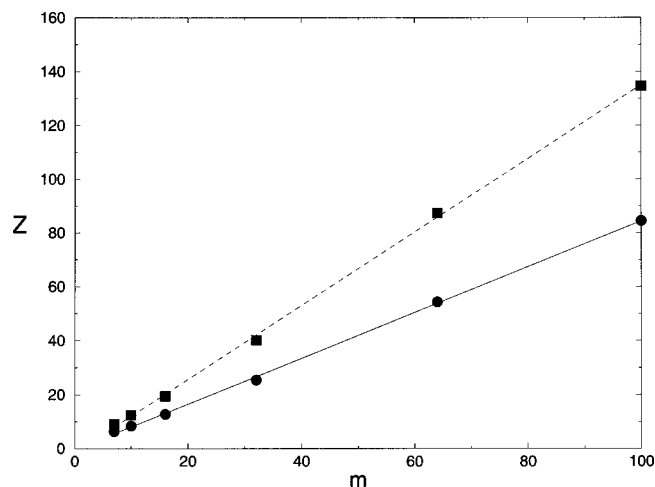


FIG. 10. Compressibility factor of the pearl-necklace model as given by the truncated virial expansion for  $y=0.20$  (circles and solid line) and for  $y=0.25$  (squares and dashed line). The lines serve as a guide to the eye and were obtained by a least-squares fit.

polymer molecules. Notice that this means that for a fixed volume fraction, pressure becomes independent of chain length. This linear dependence of  $Z$  with  $m$  appears also in almost all theoretical EOS such as Wertheim's TPT1 or the generalized Flory dimer theory. Let us analyze if the truncated virial expansion can reproduce this behavior at low pressures. In Fig. 10, the compressibility factor as obtained from the truncated virial expansion is shown as a function of  $m$  for two values of  $y$ , namely  $y=0.20$  and  $y=0.25$ . As can be seen, the truncated virial sum is able to reproduce the linear behavior of  $Z$  with  $m$  for these two volume fractions. In fact, the correlation coefficient of the linear fit is of the order of 0.9997 for both densities. It is somewhat surprising that the virial sum is able to reproduce this linear behavior, since the exact virial coefficients are not linear functions of  $m$  (see, Figs. 2–4). Because of this, one may suspect that for longer chains the truncated virial expansion will fail to reproduce the linear behavior of  $Z$  with  $m$  found in computer simulations.

Although for the chain lengths considered in this work the truncated virial expansion describes quite well the EOS for values of  $y$  less than 0.30, there is still an issue that should be mentioned. For  $m=1, 7$ , and  $16$ , the virial sum underestimates the value of  $Z$  for  $y=0.30$ . However, this is not the case for  $m=64$ , where the truncated virial sum overestimates the value of  $Z$  (see Fig. 9). It is difficult to explain why the virial sum provides a compressibility factor higher than the experimental value obtained from MC. One possible explanation is that the neglected virial coefficients (i.e., fifth, sixth, and higher) are negative, so the compressibility factor is overestimated by the virial sum. Although we cannot completely rule out this possibility, we do not think this is the case (at least for  $m=64$ ). In our view, the strange behavior found for  $m=64$ , where the virial sum gives higher values of  $Z$  than the MC simulations, is related to the conformational changes that occur in a polymer melt as the density increases.<sup>45</sup> Note that we are evaluating the virial coefficients by using configurations obtained at zero density. These con-

TABLE III. Second, third, and fourth virial coefficients for the SW pearl-necklace model described in the text. The reduced temperature  $T^* = T/(\epsilon/k)$  is 3, and  $\lambda=1.5$ . The numbers in parentheses gives the uncertainty of the last digits. Values of the mean-square radius of gyration  $\langle s^2 \rangle$  are given in the last column.

$m$	$B_2^*$	$B_3^*$	$B_4^*$	$\langle s^2 \rangle$
32	20.98(8)	213(2)	865(20)	9.473
64	30.24(9)	430(5)	2165(30)	20.508

figurations, however, are not representative of the actual configurations presented by a chain in the fluid state at nonzero density. Actually, configurations obtained at zero density are more expanded than in the melt (i.e., the square radius of gyration is larger at zero density than at liquid-like densities).<sup>45</sup> Only theories including self-consistency (namely the possibility of including conformational changes with density) can be successful in reproducing the low and high density regime of polymer molecules. Notice that this is a specific feature of hard flexible molecules. For hard rigid models, the introduction of the exact values of the first virial coefficients guarantees the agreement between the virial expansion and simulation at low densities. For hard flexible molecules, however, this is not the case. Self-consistency should be included in any theoretical treatment where the singlet correlation function is density dependent. A similar problem where this also occurs is in the case of nematogens. The virial expansion does not guarantee an exact description of the fluid once the nematic phase appears (i.e., when the singlet correlation functions becomes anisotropic).<sup>46–48</sup>

To summarize, Fig. 9 illustrates that the virial expansion provides a reasonable approximation to the EOS of the pearl-necklace model with  $m$  less than 100 and  $y$  less than 0.25, but even though we have used the exact first four virial coefficients, the agreement with simulation is not perfect because we are not properly accounting for the possibility of conformational changes in the fluid phase. It is somewhat frustrating that the virial sum does not guarantee exact behavior in the EOS even for low densities (i.e.,  $y$  less than 0.20).

In order to assess the impact of conformational changes on the virial coefficients and on the equation of state of a hard flexible model, we have evaluated the virial coefficients for a model related with the pearl-necklace model. In this new model, the intermolecular interactions are of the hard-sphere type (as in the pearl-necklace model). However, interaction between sites of the same chain will be given by the square well potential with  $\lambda=1.5$ . We shall denote this new model as the SW pearl-necklace or more briefly the SW model.

In Table III, the virial coefficients of the SW pearl-necklace model with  $m=32$  and  $64$  are given for a reduced temperature  $T^* = T/(\epsilon/k) = 3$ . For this temperature, the chains adopt more compact configurations than in the pearl-necklace model, so one can analyze the impact of the intramolecular configurations on the virial expansion and the EOS. As can be seen, the value of the second and third virial coefficient is reduced with respect to the pearl-necklace model. However, the fourth virial coefficient remains almost

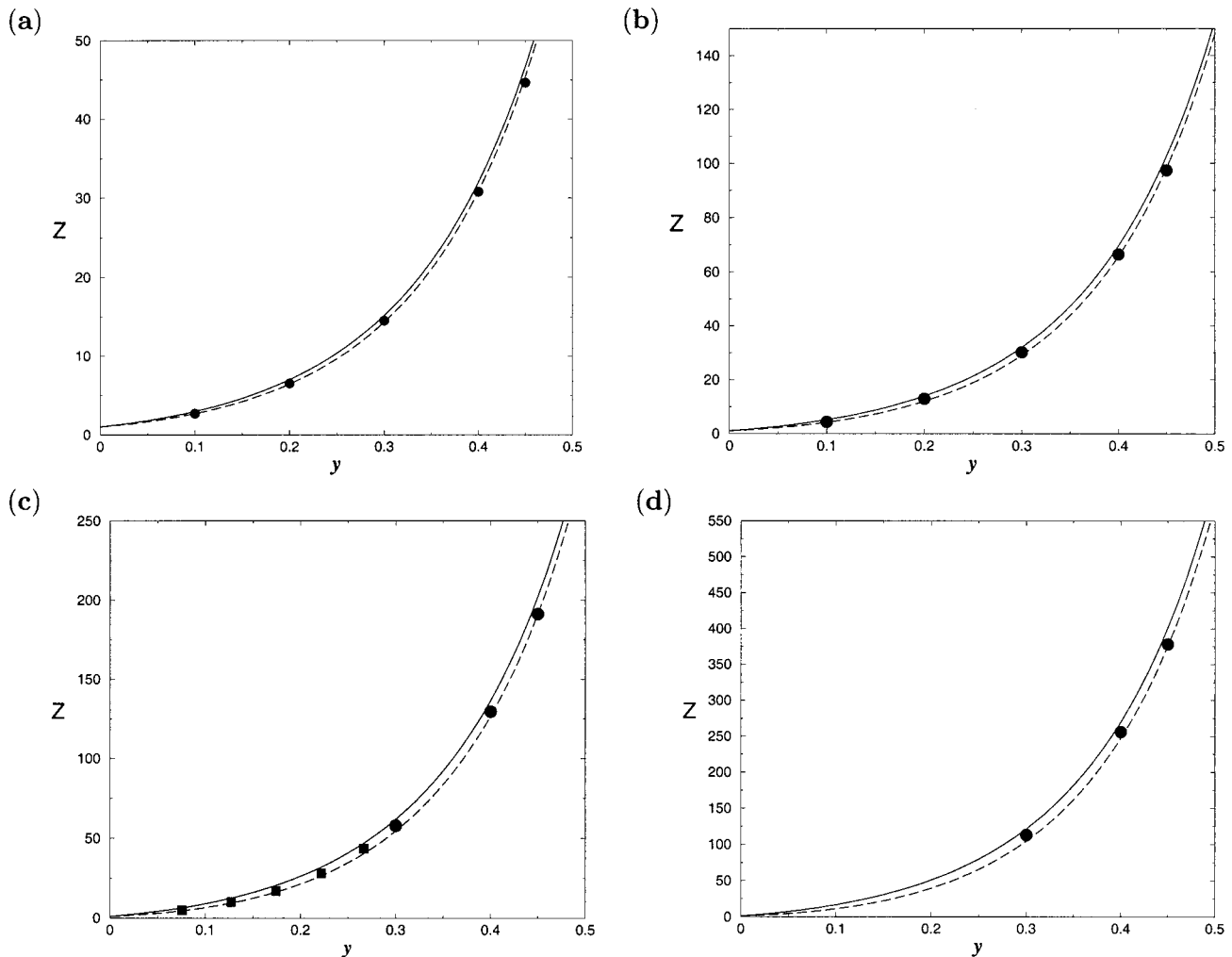


FIG. 11. Results of the EOS of the pearl-necklace model as obtained from simulation (symbols), from TPT1 (solid line), and from virial-TPT1 (dashed line) for  $m=7,16,32,64$ . (a) Results for  $m=7$ . (b) Results for  $m=16$ . (c) Results for  $m=32$ . (d) Results for  $m=64$ .

the same for  $m=32$  and increases slightly for  $m=64$  (compare the data of Tables I and III). In Figs. 9(b), 9(c), the EOS for the pearl-necklace model as obtained from simulation, from the virial expansion, and from the virial expansion of the SW model are shown. As can be seen, the shape of the molecule affects the equation of state. In the pearl-necklace model, the radius of gyration in the melt is somewhere between that of the pearl-necklace model at zero density and that of the SW model at zero density. The results of Figs. 9(b), 9(c) again give evidence that only self-consistent theories can successfully describe the EOS of a flexible molecule in all the range of densities.

Finally, we would like to propose a new EOS for the pearl-necklace model. TPT1 is a good EOS for the pearl-necklace model at high densities. However, it overestimates substantially the pressure at low densities. One may expect that the introduction of the correct virial coefficient in TPT1 will result in an improved EOS. This kind of correction was introduced by Yethiraj *et al.*<sup>14</sup> for the generalized Flory dimer theory. One would expect that the same correction can be applied for TPT1. A similar treatment combining low and high density EOS has also been proposed recently by Lue.<sup>39</sup> Therefore, we shall use TPT1 but imposing the correct con-

tribution arising from the second virial coefficient. This new equation, which we will denote as virial-TPT1, reads as follows:

$$Z = Z_{\text{TPT1}} + (B_2^* - B_2^{*,\text{TPT1}})y, \quad (20)$$

where  $Z_{\text{TPT1}}$  and  $B_2^{*,\text{TPT1}}$  are given by Eqs. (5)–(6), respectively, and  $B_2^*$  is the exact reduced second virial coefficient as obtained numerically in this work. In Fig. 11, the results of this EOS for  $m=7, 16, 32$ , and  $64$  are compared to simulation results. As can be seen, virial-TPT1 significantly improves the results of TPT1, not only at low but also at high densities.

## V. CONCLUSIONS

In this work, the second, third, and fourth virial coefficients of the pearl-necklace model with up to 100 monomer units have been computed. To our knowledge, this is the first time that the third and fourth virial coefficients of a polymer in the continuum have been computed. Preliminary results for  $m=150$  and  $m=200$  have also been given. We have computed the virial coefficients for a linear rigid model to assess the impact of flexibility on the virial coefficients. The

results provided in this article may be useful for researchers looking for an EOS of the pearl-necklace model.

We can summarize the following conclusions from this work.

(1) Virial coefficients of flexible and rigid molecules differ significantly. Only the third virial coefficient seems to be insensitive to the existence or absence of flexibility. The second and third virial coefficients of flexible and rigid models increase with the chain length (although not linearly). However, the fourth virial coefficient seems to reach a maximum and then goes to negative values, for both rigid and flexible chains.

(2) Wertheim's EOS does not accurately predict the virial coefficients neither for the pearl-necklace model nor for the rigid linear chain. It overestimates  $B_2$  and underestimates  $B_3$  and  $B_4$ . At very low densities, where  $B_2$  is dominant, Wertheim's EOS overestimates the pressure. However, at medium densities, where the effects of  $B_3$  and  $B_4$  are significant, some cancellation of errors occurs and Wertheim's EOS yields acceptable results.

(3) As expected, virial coefficients of the rigid linear tangent hard sphere model present Onsager's scaling. For the pearl-necklace model, the second and third virial coefficient present de Gennes' scaling and the results of this work suggest that the fourth virial coefficient presents Onsager scaling.

(4) Using mixing rules for the crossed virial coefficients is an approximate method of estimating the virial coefficients of a polymer. This method yields good results for the second and third virial coefficient but fails for the fourth.

(5) The approximate method allows us to establish certain correlations between geometrical magnitudes of the pearl-necklace model. In particular, it is shown that  $B_3$  and  $B_2$  are strongly correlated, and also  $B_4$  and  $s^2$ . Configurations with large values of  $s^2$  are somewhat stretched and present negative values of  $B_4$ .

(6) The virial expansion provides a reasonable EOS for the pearl-necklace model for volume fractions up to  $\gamma = 0.25$ . However, for long chains the virial expansion overestimates the pressure even for densities less than  $\gamma = 0.25$ . The reason is that the virial expansion does not account for the conformational changes that occur in the melt, even at these low densities. Virial coefficients are calculated using configurations of the model at zero density, which are not representative of the configurations adopted by the chain in the melt.

(7) Virial coefficients and the EOS are sensitive to conformational changes. When intramolecular interactions are replaced by square-well interactions, the chain is somewhat more folded. This affects the value of the virial coefficients and the EOS. In fact, the compressibility factor of SW pearl-necklace chains is lower than that of the pearl-necklace model.

(8) The search for a successful EOS for the pearl-necklace model in the low and high density limit requires the introduction of self-consistency. One could probably obtain a successful EOS for densities smaller than  $\gamma = 0.25$  by combining the virial expansion with a theory which allow conformational changes with density.

(9) It is shown that TPT1 can be improved by simply introducing the correct value of the second virial coefficient. That improves significantly the results for low densities, and slightly for high densities for chains from 7 up to 64 monomer units.

## ACKNOWLEDGMENTS

Financial support is due to Project No. PB97-0329 of the Spanish DGICYT (Dirección General de Investigación Científica y Técnica). We thank the "Centro de Supercomputación" of Universidad Complutense de Madrid for a generous allocation of computer time in the 32 processor parallel machine Seymour 2000, within the project "Determinación de coeficientes del virial de polímeros." We also thank Dr. Carl McBride for providing us with the MC data of the pearl-necklace model with  $m = 32$ . Helpful discussions with Professor J. J. Freire are gratefully acknowledged.

- <sup>1</sup>R. Dickman and C. K. Hall, *J. Chem. Phys.* **85**, 4108 (1986).
- <sup>2</sup>R. Dickman and C. K. Hall, *J. Chem. Phys.* **89**, 3168 (1988).
- <sup>3</sup>J. Chang and S. I. Sandler, *Chem. Eng. Sci.* **49**, 2777 (1994).
- <sup>4</sup>A. P. Malanoski and P. A. Monson, *J. Chem. Phys.* **110**, 664 (1999).
- <sup>5</sup>M. S. Wertheim, *J. Chem. Phys.* **87**, 7323 (1987).
- <sup>6</sup>W. G. Chapman, G. Jackson, and K. E. Gubbins, *Mol. Phys.* **65**, 1057 (1988).
- <sup>7</sup>K. G. Honnell and C. K. Hall, *J. Chem. Phys.* **90**, 1841 (1989).
- <sup>8</sup>Y. C. Chiew, *Mol. Phys.* **70**, 129 (1990).
- <sup>9</sup>A. Yethiraj and C. K. Hall, *J. Chem. Phys.* **93**, 5315 (1990).
- <sup>10</sup>J. G. Curro and K. S. Schweizer, *J. Chem. Phys.* **87**, 1842 (1987).
- <sup>11</sup>Y. C. Chiew, *Mol. Phys.* **73**, 359 (1991).
- <sup>12</sup>J. Chang and S. I. Sandler, *J. Chem. Phys.* **102**, 437 (1995).
- <sup>13</sup>C. T. Lin, G. Stell, and Y. V. Kalyuzhnyi, *J. Chem. Phys.* **112**, 3071 (2000).
- <sup>14</sup>A. Yethiraj, K. G. Honnell, and C. K. Hall, *Macromolecules* **25**, 3979 (1992).
- <sup>15</sup>J. M. Wichert and C. K. Hall, *Macromolecules* **27**, 2744 (1994).
- <sup>16</sup>C. Vega, *Mol. Phys.* **98**, 973 (2000).
- <sup>17</sup>W. Bruns, *Macromolecules* **30**, 4429 (1997).
- <sup>18</sup>D. A. McQuarrie, *Statistical Mechanics* (Harper & Row, New York, 1976).
- <sup>19</sup>J. P. Hansen, and I. R. McDonald, *Theory of Simple Liquids*, 2nd ed. (Academic, New York, 1986).
- <sup>20</sup>C. G. Gray and K. E. Gubbins, *Theory of Molecular Fluids* (Clarendon, Oxford, 1984).
- <sup>21</sup>F. H. Ree and W. G. Hoover, *J. Chem. Phys.* **40**, 939 (1964).
- <sup>22</sup>M. P. Allen and D. J. Tildesley, *Computer Simulation of Liquids* (Clarendon, Oxford, 1987).
- <sup>23</sup>T. Boublik, *Mol. Phys.* **68**, 191 (1989).
- <sup>24</sup>T. Boublik, C. Vega, and M. Diaz Pena, *J. Chem. Phys.* **93**, 730 (1990).
- <sup>25</sup>C. Vega, B. Garzon, and S. Lago, *Mol. Phys.* **82**, 1233 (1994).
- <sup>26</sup>P. G. de Gennes, *Scaling Concepts in Polymer Physics* (Cornell University Press, Ithaca, 1979).
- <sup>27</sup>A. M. Rubio and J. J. Freire, *Macromolecules* **29**, 6946 (1996).
- <sup>28</sup>W. Bruns, *Macromolecules* **29**, 2641 (1996).
- <sup>29</sup>L. G. MacDowell and C. Vega, *J. Chem. Phys.* **109**, 5670 (1998).
- <sup>30</sup>D. C. Williamson and G. Jackson, *Mol. Phys.* **86**, 819 (1995).
- <sup>31</sup>K. M. Jaffer, S. B. Opps, and D. E. Sullivan, *J. Chem. Phys.* **110**, 11630 (1999).
- <sup>32</sup>H. Fujita, *Polymer Solutions* (Elsevier, Amsterdam, 1990).
- <sup>33</sup>P. J. Flory, *Principles of Polymer Chemistry* (Cornell University Press, Ithaca, 1953).
- <sup>34</sup>G. C. Berry, *J. Chem. Phys.* **44**, 4550 (1966).
- <sup>35</sup>J. F. Douglas and K. F. Freed, *Macromolecules* **18**, 201 (1985).
- <sup>36</sup>J. des Cloizeaux and J. Noda, *Macromolecules* **15**, 1505 (1982).
- <sup>37</sup>D. Frenkel, *J. Phys. Chem.* **92**, 5314 (1988).
- <sup>38</sup>L. Onsager, *Ann. N.Y. Acad. Sci.* **51**, 627 (1949).
- <sup>39</sup>L. Lue, *J. Chem. Phys.* **112**, 3442 (2000).
- <sup>40</sup>J. M. Labaig, Masters thesis, Universidad Complutense de Madrid, 1999.

- <sup>41</sup>T. Boublik and I. Nezbeda, *Collect. Czech. Chem. Commun.* **51**, 2301 (1986).  
<sup>42</sup>P. A. Monson and M. Rigby, *Mol. Phys.* **35**, ■■ (1978).  
<sup>43</sup>C. Vega, *Mol. Phys.* **92**, 651 (1997).  
<sup>44</sup>Y. Zhou, S. W. Smith, and C. K. Hall, *Mol. Phys.* **86**, 1157 (1995).  
<sup>45</sup>A. J. Haslam, G. Jackson, and T. C. B. McLeish, *J. Chem. Phys.* **111**, 416 (1999).

- <sup>46</sup>G. J. Vroege and H. N. W. Lekkerkerker, *Rep. Prog. Phys.* **55**, 1241 (1992).  
<sup>47</sup>P. Padilla and E. Velasco, *J. Chem. Phys.* **106**, 10299 (1997).  
<sup>48</sup>E. Velasco and P. Padilla, *Mol. Phys.* **94**, 335 (1998).  
<sup>49</sup>■. McBride (private communication).

PROOF COPY 509046JCP